Sustainable Cities and Society 46 (2019) 101407

Contents lists available at ScienceDirect

Sustainable Cities and Society

journal homepage: www.elsevier.com/locate/scs

A method proposal for monitoring the microclimatic change in an urban area

Çağdaş Kuşçu Şimşek*, Halime Ödül

Geomatics Engineering, Sivas Cumhuriyet University, Sivas, Turkey

ARTICLE INFO

Keywords:
Micro-climate
Urban planning
Change detection
GIS
Remote sensing
Modeling

ABSTRACT

It is known that changes in urban surface characteristics lead to different urban climates. The surrounding environment directly affects thermal comfort and human behavior. In this respect, for sustainable urban growth, the evaluation of urbanization together with climate change from past to present is also important for planning.

The main aim of the study is to propose a retrospective GIS-based change detection method for the monitoring of urban climate change by using satellite images. Two regions with a diameter of 1 km where there are significant constructional changes in Istanbul were selected as the study areas. The comparisons were made through Landsat thermal images during summer between the years 2007 and 2017. The function of the model proposed in the study was tested by evaluating whether the expected climatic changes could be achieved against the constructional changes that took place in the region. The correlations between the regions that get extremely hot / cold and the constructional change areas were examined by the bivariate method. The results showed that the correlations could reach up to a high level when important changes occurred in the areas.

1. Introduction

A sustainable urban growth must be intended least dependency on natural resources and non-renewable energy. But on the other hand, the expansion of urban area and the increase in urban population brings huge challenges for the planners to provide a sustainable urbanization due to the more energy requirement issues and environmental issues (Wang, Ma, Ding, & Liang, 2018; Wang, Ren, Xu, Lau, & Shi, 2018).

Urban systems affect the energy absorption, release, and the climate. The thermal balance of the urban area is explained by the balance between the heat gained from the sun and the heat loss released by longwave radiation. This is a complex system depending on many environmental factors, such as solar radiation, cloud cover, wind speed, soil moisture, and land surface type (Zhang et al., 2015). So, expansion of urban area, i.e., the increase of impervious surface area having relatively higher LST amplified the scope of the urban heat island, which may be further lead to the increase of air temperature in a long time period (Wang, Ma et al., 2018; Wang, Ren et al., 2018). Therefore, the urban climate characteristics, and the heat and wind distribution depending on the morphological characteristics of the city should be very well understood for the effective design of the urban area (Bernard, Rodler, Morille, & Zhang, 2018; Tong et al., 2018; Tsoka, Tsikaloudaki, & Theodosiou, 2017; Yahia, Johansson, Thorsson, Lindberg, & Rasmussen, 2018). Especially in urban centers, high temperatures that disturb the urban population due to dense and high housing or the formation of unusual wind corridors due to incorrectly designed streets and high-rise buildings are the most common problems (Gabriel & Endlicher, 2011; Tong et al., 2017).

Theoretical studies, terrestrial measurements, and satellite data that have been done for many years reveal the climatic changes to which cities are exposed (Coutts, Beringer, & Tapper, 2007; Levermore, Parkinson, Laycock, & Lindley, 2014; Linh & Chuong, 2015; Koc, Osmond, & Peters, 2018; Wang, Ma et al., 2018; Wang, Ren et al., 2018; Wang, Berardi, & Akbari, 2015). There are also many studies on the investigation of the parameters that trigger this situation (Lin, Lau, Qin, & Gou, 2017; Srivanit & Kazunori, 2011; Tornay, Schoetter, Bonhomme, Faraut, & Masson, 2017; Wang, Berardi, & Akbari, 2016; Wong, Jusuf, & Tan, 2011). In these studies, it is observed that urban sprawl (Guo-Yu, 2015; Roshan, Rousta, & Ramesh, 2009), population size and population growth rate (Petkova et al., 2017; Wang & Wang, 2017), urban morphology (Xu et al., 2017), urban density, vegetation cover (Estoque, Murayama, & Myint, 2017; Herrera-Gomez, Quevedo-Nolasco, & Pérez-Urrestarazu, 2017; Upreti, Wang, & Yang, 2017), urban surface characteristics (Mackey, Lee, & Smith, 2012; Morakinyo, Dahanayake, Ng, & Chow, 2017; Salata et al., 2017) direction/velocity of wind (Levermore, Parkinson, Lee, Laycock, & Lindley, 2017; Wang &

* Corresponding author.
E-mail address: cksimsek@cumhuriyet.edu.tr (Ç. Kuşçu Şimşek).

https://doi.org/10.1016/j.scs.2018.12.035
Received 24 August 2018; Received in revised form 25 December 2018; Accepted 27 December 2018
Available online 03 January 2019

Akbari, 2016), consumption habits (Heinonen & Junnila, 2011; Sudmant, Gouldson, Millward-Hopkins, Scott, & Barrett, 2018) and lifestyle (Rehdanz & Maddison, 2005; Roy & Pal, 2009) are the most important factors in urban climate change.

Urban morphology describes the form, shape, plan, structure, and functions of the texture of cities. In this context, the geometrical and functional relations of buildings, which are one of the urban climate parameters, are evaluated under urban morphology. Building layout geometry, orientation, and material composition have significant influences on indoor and outdoor climate (Lin, Lau et al., 2017).

In the studies on climate with a varying and complex structure depending on many factors, the determination of factors effects and the evaluation of research results become difficult due to the effects of side factors. The way to evaluate these complex relationships in a precise way is based on the choice of a right method and a right scale. Climate change varies by the scale as well as temporal and spatial differences (Şen, 2009). The climatic scale, which varies by the national, regional and local scale, comes to the forefront as a strategically decisive criterion. Grimmond et al. (2010) divided scaling into three in urban climate studies. According to this classification, the city and region scale was defined as meso, the neighborhood scale was defined as local, and the street scale was defined as micro. In the studies on urban climate, data are obtained by terrestrial station measurements, mobile measurements, and remote sensing techniques. The choice of the method varies by the aim, scale, spatial and temporal characteristics of the study.

Despite the complexity of the spatial and spectral diversity of urban environment, remote sensing techniques can be used to measure, limit, and classify different urban environments with different resolutions. Especially the use of time series satellite images allows for more accurate monitoring and understanding of the past and development despite the complexity of urban dynamics (Weng & Quattrochi, 2007). The advantages of using this technique are that it is capable of visualizing the temperature of large areas and that the huge amount of thermal data can be obtained at a time (Sabnis, 2011). The omission of green cover under trees and wall temperatures by measuring surface temperatures from an aerial viewpoint weakens the method (Voogt & Oke, 1997). However, there are many studies indicating a high correlation between surface temperatures and air temperatures (Benali, Carvalho, Nunes, Carvalhais, & Santos, 2012; Widyasamratri et al., 2013; Zhang et al., 2015; Hadria et al., 2017). Therefore, the information obtained by remote sensing data also indicates the climatic structure of the city.

For a sustainable urban growth, it is important to develop planning strategies by monitoring the change from past to present and determining the causes of this change accurately. In this respect, the use of remote sensing techniques is provided convenience to following the past and following the temporal changes. By means of remote sensing techniques, changes that take place in the region can be monitored through the images of two or more periods of time of the same geographical region (Ferraris, Dobigeon, Wei, & Chabert, 2018; Guo-Yu, 2015). In particular, change detection analyses used for detecting and monitoring environmental changes, disasters, and land use changes are important in terms of sustainability (Nsubuga et al., 2015).

In the literature, there are numerous examples of spatio-temporal change detection (Hulley, Veraverbeke, & Hook, 2014; Liu, Bruzzone, Bovolo, & Du, 2015; Lu, Li, & Moran, 2014; Zhu & Woodcock, 2014; Zhu, 2017). However, most of the change detection methods cannot be used in thermal bands (climatic research) since they are based on the examination of the change in the reflectance value of each pixel (Guo-Yu, 2015; Hao, Hua, Li, & Chen, 2017). This situation which is due to the fact that the numerical change in thermal band pixels does not reflect a climatic change (in the way that the air temperature which is t today will be t ± n tomorrow) requires the creation of a model for the monitoring of climatic changes through satellite images. With respect to the models related to climatic change detection analysis in literature (Manogaran and Lopez; 2018; Katzfuss, Hammerling, & Smith, 2017), there is a limited number of studies.

With this study, a geographic information system (GIS) based, an easy change detection method is proposed for the retrospective monitoring of temporal temperature changes that are difficult to compare through satellite images directly. In the study, the surface temperature data of all years obtained from satellite images were collected in a database. The analyses were performed through this database.

In the study in which the regions that get extremely hot/cold each year between 2007 and 2017 were determined based on the year 2007, the selected two regions where there are significant constructional changes were analyzed. The results obtained were compared with the constructional changes that took place in this period of time. The function of the model proposed in the study was tested by evaluating whether the expected climatic changes could be achieved against the constructional changes that took place in the region.

This study proposes an easy modeling method that can be applied manually with the help of GIS techniques. The results of the study reveal that it is possible to monitor the regional climate changes with the proposed method. With this method, target points can be determined for more precise investigations by marking the change/problem points determined through satellite images. The strategies to be developed through these data are important for the healthy development of the city. Sustainable urban development is based on the accurate interpretation of the past and the present.

2. Materials and methods

2.1. Study area

It is known that there have been various constructional changes in Şişli and Beşiktaş districts of Istanbul province since 2007. The most important one of these is the demolition of Ali Sami Yen stadium in 2011 and then the construction of a 42-storey skyscraper (Torun Center) built on 39.000 m^2 plot area with the residence, office and shopping area. Another one is the mix-used building complex (Zorlu Center) with 4 residential towers, shopping center, hotel and performance arts center built on 102.000 m^2 plot area.

These regions were decided to be selected as the study areas by considering that these changes and other constructional changes around them would also lead to significant changes in the microclimate structure of the regions (Fig. 1). 1 km perimeters of Torun Center and Zorlu Center were determined as the study areas. Detailed information about the projects carried out within the study areas are presented in Table A.1 and Table A.2.

2.2. Data

Landsat ETM –7 (2007–2014) and Landsat 8 (2015–2017) satellite images were used as data in this study. The images cover the years between 2007 and 2017, and the images of the recent period were preferred to minimize the effects of seasonal differences in the choice of images. The study was carried out during the summer period so that regional warming could be detected more easily. The image dates are June 4 2007, July 8 2008, June 25, 2009, June 12, 2010, July 17, 2011, June 17, 2012, June 6 2013, July 9 2014, July 12, 2015, July14 2016, July 1 2017, respectively. The average air temperatures for Istanbul measured on image dates are presented in Table 1. Comparisons of the surface temperatures of study areas with the air temperature of Istanbul were given in Figure A.1 and Figure A.2.

2.3. Method

In this study, the main problem attempted to be solved by a method proposal is that daily temperature changes compared do not indicate a microclimatic change; therefore, there is a need for developing a model

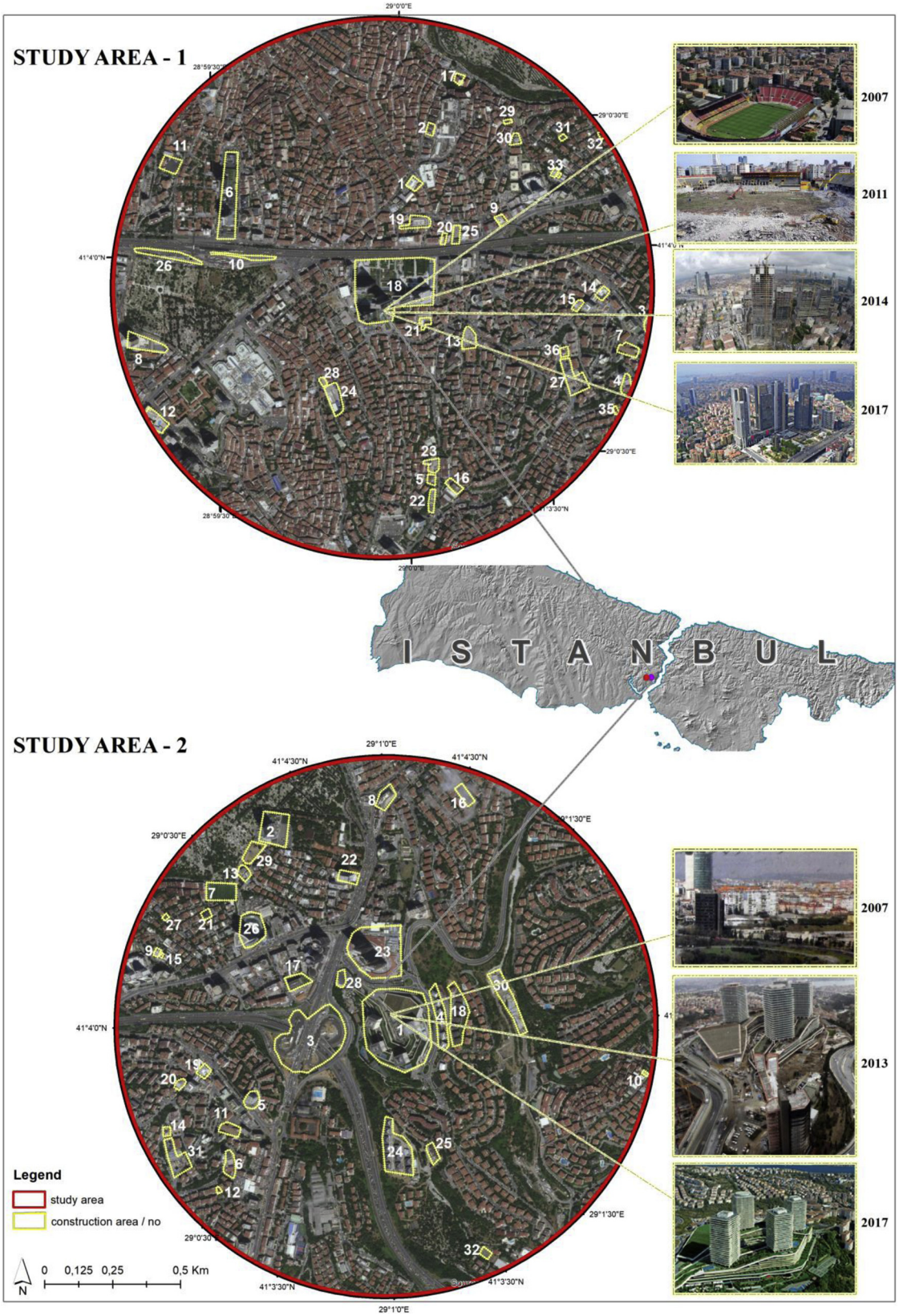

Fig. 1. Study Area–1, Study Area–2 and construction areas.
(The photographs are taken from Fotomaç, 2018; Cnnturk, 2011; Cnnturk, 2014; Corpneed, 2018; Emlak Kulisi, 2018; Arkitera; 2013; Zorlu Grup, 2018)

Table 1
Average air temperatures of Istanbul measured on image dates.

Date	04.06.2007	08.07.2008	25.06.2009	12.06.2010	17.07.2011	17.06.2012	06.06.2013	09.07.2014	21.07.2015	14.07.2016	01.072017
Mean air temperatures for Istanbul	29 C°	30 C°	29 C°	30 C°	35 C°	28 C°	25 C°	31 C°	29 C°	31 C°	38 C°

to be able to compare the surface temperatures to be obtained from images in terms of a microclimatic change. In other words, the fact that the air temperature is 29 °C on the date of t + 1 or 20 °C on the date of t + 2 while it is 23 °C on the date of t does not indicate a climatic difference depending on the anthropogenic changes of the region. So, a comparison cannot be made (in terms of determining the regions that get hot or cold) by directly dealing with the surface temperatures obtained from satellite images.

So, the main aim of the study is to propose a GIS-based change detection method for the monitoring of urban climate change by using satellite images. The method is based on the comparison of surface temperature information of different periods obtained through satellite images with the help of a model created in the GIS environment. The change detection method used in the study represents only image days. Since the method is based on the differences of two images, two images can be used in any range. In this study, the time interval which is known to have differences between the two images (1 year for this sample) was taken as a sampling method.

In the study, since retrospective climatic controls could not be performed by terrestrial measurements, the control mechanism of the method was formed through "constructional changing areas", which is one of the influential factors on urban climate. Hence, the accuracy of the method was tested based on the literature information on urban climate change and by considering the expected climate changes as a result of constructing within the region. However, in order to reveal this relationship, it was tested by the bivariate correlation analysis at a significance level of 0.01 whether a constructional change is related to extreme warming and cooling in the region. So, construction data used in the project are the side data used to control the accuracy of the method. For this reason, the correlation analyses of building factors (floor, floor area, facade materials, etc.) were not performed, and evaluations were made based on verbal literature information.

The issue of climate is a multi-parameter research area that is evaluated with different details at different scales. Therefore, studies on this issue with a varying and complex structure depending on many factors also become difficult due to the effects of other factors. At this point, the right choice of the research scale, period and method is important for the accuracy of evaluation.

In this study which was carried out during summer on a micro scale, the measurements and evaluations were performed with the help of remote sensing and GIS techniques. Micro-scale climate studies are carried out by terrestrial measurements or remote sensing methods. The main difference between two methods is that air temperatures are examined by terrestrial measurements while surface temperatures are examined by remote sensing studies. Since temporal change would be examined in this study, remote sensing data were used since they allow obtaining thermal data of the previous years, obtaining synchronous thermal data of the entire study area through the image of a single period, and thus, the holistic evaluation of the region.

Spectral radiance values are gathered by using sensor calibration parameters in order to obtain surface temperatures through thermal imagery when evaluating the satellite images. Thermal data were corrected, according to the Landsat 7 ETM (Chander, Markham, & Helder, 2009) and Landsat 8 radiometric calibration parameters (USGS, 2018), before starting the image processing studies. Then, the NDVI (normalized difference vegetation index) and ε (emissivity) values, which make the reflection qualities of surface elements clear, were calculated. The emissivity values changes, due to the surface roughness, vegetation cover etc. In this study, to estimate the different land surfaces emissivity values, NDVI threshold method (NTM) was used which was formulated by Sobrino et al. (2008). Then, according to the radiative transfer equation, which was used by Jiménez-Muñoz et al. (2009), the radiation brightness values are calculated. Lastly, surface temperatures are calculated separately for all thermal images.

Thus, the surface temperatures obtained through time series satellite images were taken into the GIS environment in pixel detail. In the study, the image of the year 2007 was selected as the reference data, and the images of the other years were used as comparison data. Single data was generated by associating the reference image with the temperature data of other years to be able to compare all temperature data with each other and to make the necessary calculations.

If the model is mathematically exemplified for the determination of areas that get hot;

Reference image surface temperatures: Ts_{2007}

Comparison image surface temperatures: Ts_{2017}

$$Ts_{2007} = \{x_1,x_2,x_3,x_4,x_5,x_6,...\} \qquad Ts_{2017} = \{y_1,y_2,y_3,y_4,y_5,y_6,...\}$$
$$Ts_{2007(Average)} = \sum Ts_{2007}/\, n(Ts_{2007}) = X \qquad Ts_{2017(Average)} = \sum Ts_{2017}/\, n(Ts_{2017}) = Y \quad (1)$$

For Ts_{2007}; $x_n < X \rightarrow C=1$ $\quad x_n > X \rightarrow C=0$ $\quad C=\{1,0,0,1,1,.....\}$

For Ts_{2017}; $y_n < Y \rightarrow H=0$ $\quad y_n > Y \rightarrow H=1$ $\quad H=\{1,0,0,0,1,.....\}$

$C_1 = 1 <=> H_1 = 1 \rightarrow A = 1$

In this way, cluster A consisting of the study data was obtained. Subsequent operations were performed through cluster A. The opposite of the Eq. (1) is used to determine the cluster of cold areas (see Eq. (B.1)).

Ts_{2007} and Ts_{2017} averages were compared for the second time for cluster A data selected. According to this comparison, X' and Y' averages were obtained (Eq. (2)). The reason for the second averaging was that the image with the high temperature average would be divided by the other while performing the image proportioning. Since the average would change due to the extracted data in the first stage, the comparison was made by performing averaging for the second time.

$$Ts_{2007(Average)} = \Sigma Ts_{2007} / n(Ts_{2007}) = X' \; Ts_{2017(Average)} = \Sigma Ts_{2017} / n(Ts_{2017}) = Y' \quad (2)$$

According to the correlation between X' and Y' values, the proportional values between the comparison image and the reference image were obtained (Eq. (3)).

$$X'>Y' \rightarrow R_n = x_n/y_n$$
$$Y'>X' \rightarrow R_n = y_n/x_n \quad (3)$$

Within the cluster R obtained, it was accepted that the larger R_n was, the higher warming was. The *Mahalanobis distance* method, which is used in the analysis of extreme values in statistics, was used to determine these extreme values within cluster R. Extreme values were determined by obtaining cluster D with the Mahalanobis distance calculation applied to cluster R, using the SPSS program.

The mahalanobis distance, which is a measure of the distance between each observation in a multidimensional cloud of points and the centroid of the cloud (Fig. 2). The Mahalanobis distance D^2 is given by Eq. (4); where "a" is a vector of values for a particular observation, "m" is the vector of means of each variable, and "V" is the variance-covariance matrix (Bartlein, 2017).

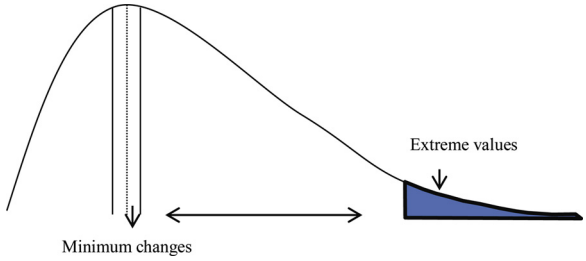

Fig. 2. Mahalanobis Distance.

$$D^2 = (a\text{-}m)V^{-1}(a\text{-}m) \quad (4)$$

Cluster D obtained was also classified in itself by the Hot Spot Analysis, and microclimatic change regions were visualized and mapped. The Hot Spot Analysis uses the Getis-Ord Gi* statistical formulation (Eq. (5)) where $\bar{X}$ is the sample mean, S is the standart deviation, and n is the number of observations (Songchitruksa & Zeng, 2010). The working principle of the method is comparing of the values of points with their neighbors. According to this method, each high value does not indicate a statistically significant region. The hot spot points show that the high-value points which have also high-value neighbors. In this method, the local sum of the point and its neighbors is compared proportionally with the sum of all points.

$$\bar{X} = \frac{\sum_{j=1}^{n} x_j}{n} \quad S = \sqrt{\frac{\sum_{j=1}^{n} x_j^2}{n} - (\bar{X})^2} \quad (5)$$

$$G_i^* = \frac{\sum_{j=1}^{n} w_{i,j}x_j - \bar{X}\sum_{j=1}^{n} w_{i,j}}{S\sqrt{\frac{\left[n\sum_{j=1}^{n} w_{i,j}^2 - \left(\sum_{j=1}^{n} w_{i,j}\right)^2\right]}{n-1}}}$$

In the final stage, correlations between the proximity of extremely hot/cold regions to the constructional change areas were examined by the bivariate method at 0.01 significance level, and then the results were evaluated. The function of the model proposed in the study was tested by examining whether the expected climatic changes could be achieved against the constructional changes using maps and statistics.

3. Results

As a result of the study, the maps of the regions that get hot and cold compared to the year 2007 were produced. In the data obtained, for the elimination of small changes among the Getis-Ord Gi* values, the values less than -1 were not accepted as a change, the values greater than -1 representing moderate and high changes were used (Figure C.1, Figure C.2, Figure C.3, Figure C.4).

When the area that gets hot, the area that gets cold, and the constructional changes were evaluated together through these maps obtained, it was observed that there were microclimatic changes in the constructional change regions in Study Area-1 and Study Area-2 (Figs. 3 and 4).

Then, this relationship was checked through statistically testing by the Bivariate correlation method at a significance level of 0.01. Correlations between the points (that get hot and cold), where the GzScore is greater than -1 (GzScore legend can be seen in Figure C.1, C.2, C.3, C.4) and their distances with the project areas are presented in Table 2. Also, the correlations between the extreme changing points (GzScore > 2) and their distances with the project areas are presented in Table 3.

When the areas that got hot/cold were evaluated according to GzScore > -1 which were given in Table 2, it was determined that there were significant correlations in a significance level of 0.01. In study area-1, after 2009, significant relationships are observed both at cold and hot points, and the relationship level reaches 0.433 and 0.527 at hot and cold points, respectively. In study area-2, hot and cold points exhibited different relationships. According to these results, the correlations reached up to 0.792 in cooled areas. However, when the statistics of heated areas were examined, a regular and significant correlation similar to cooled areas could not be found. According to this result, it was observed that the project areas affected their immediate surroundings for cooling in study area-2.

When overheated / overcooled areas are evaluated according to GzScore > 2 given in Table 3, it is observed that correlations vary. In study area-1, after 2011 (demolition of Ali Sami Yen), the correlations of overheated areas reached up to 0.809. In overcooled areas, although there were significant differences reaching 0.487 after 2012, no regular structure was observed in the relationships. In study area 2, the exact opposite situation occurred. In overcooled areas, significant relationships were found in the correlation range of 0.350-0.657 in all years except for the year 2008. In overheated areas, no regular structure was observed in the relationships.

Indeed, regional climate change has a multifactorial and complex structure. Therefore, a very high correlation is not expected when the relationship between all changes (GzScore > -1 data) in the study area is examined with a single factor (construction). However, the regions selected as the study area are the regions where significant changes have occurred along with the major changes and the climate change is expected. When the data in Table 2 evaluating all changes (GzScore > -1) in the study area are examined, it is observed that there are significant relationships between temperature changes and constructions. When the data in Table 3 (GzScore > 2 data) are evaluated, whether constructions have a heating or cooling effect on regional climate change becomes evident. It was observed that the projects conducted in study area-1 and study area-2 created a heating effect and cooling effect, respectively, in the region. Extreme changes occurring especially in large project areas reveal that such projects play an important role in regional climate change.

However, an important point to be mentioned here is that since the increase in warming or cooling occurring depending on any factor is calculated based on the regional average, it leads to the occurrence of the exact opposite situation for other areas (falling below average or rising above average). In other words, there will be points tending towards warming or cooling, so this should also be taken into consideration while evaluating the results.

When all the maps and data in Table A.1 and Table A.2 were evaluated visually together, it was observed that microclimatic change areas were associated with the projects carried out within the region. In particular, the effects of project number 18 in study area-1 and project number 1 in study-area-2 can be easily observed with the help of maps.

In the final stage, the surface temperature differences within the study areas were examined (Table 4). According to this results, it was determined that minimum and maximum surface temperature differences of study area-1 and study area-2 are reach up to 37.4 °C and 19.8 °C respectively. Upon examining for all years, it is observed that they created average differences of 26.5 °C and 11.7 °C, respectively.

When temperature differences within 100 m perimeters of the project areas were examined, it was determined that maximum temperature differences were generally observed around the skyscraper projects or in very large project areas at the base. Maximum temperature differences around the major project areas in the study areas are presented in Table 5. According to the table prepared based on the completion year of the projects, it is observed that there is a surface temperature difference of up to 26 °C around a single project area.

4. Discussion

The main aim of the model proposed in this study is to ensure the monitoring of climatic changes that take place within the city in any period of time (such as from past to present) using satellite images. The accuracy of the method was tested based on the literature information

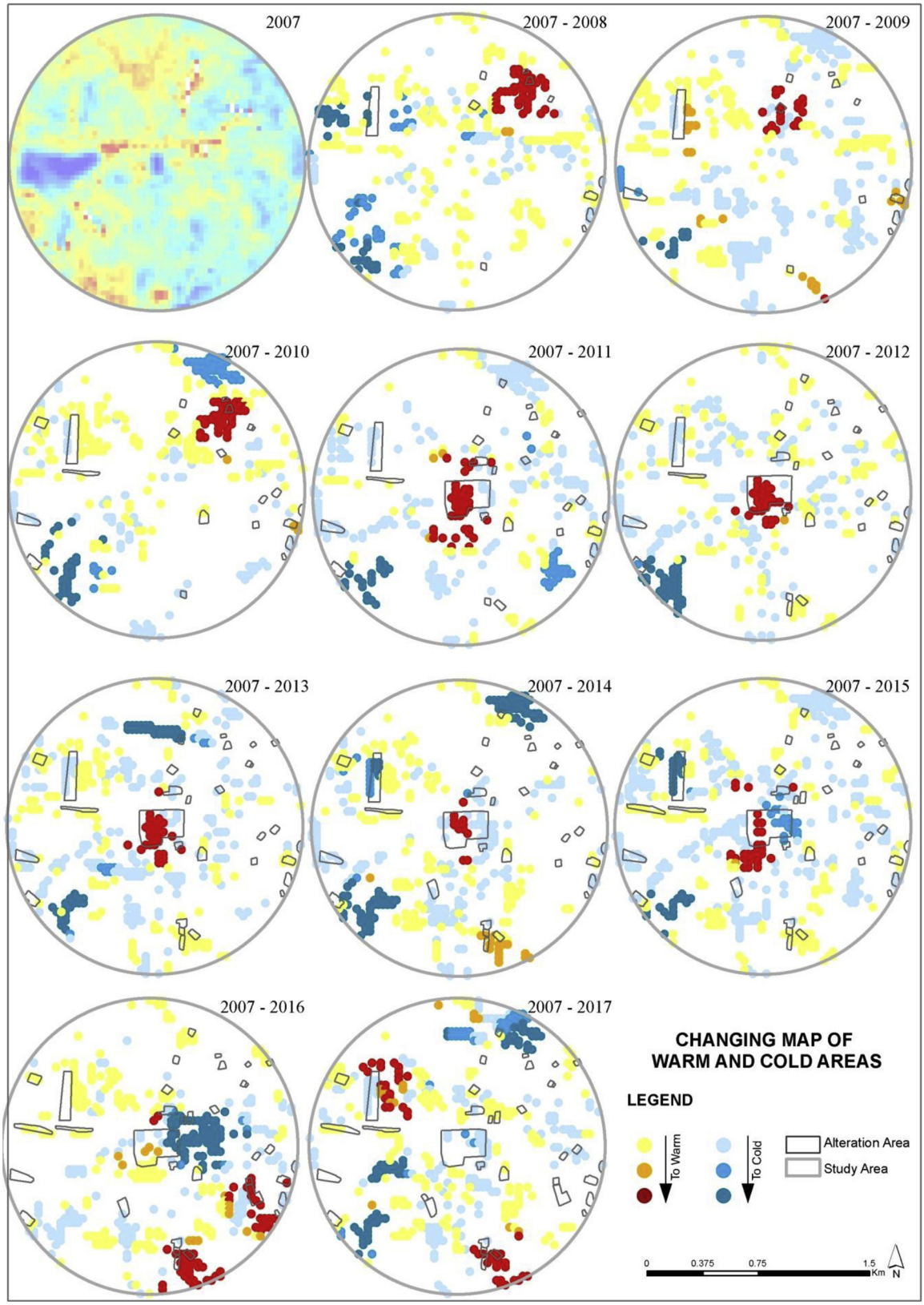

Fig. 3. Changing map of warm and cold areas for Study Area-1.

on urban climate change and by considering the expected climate changes as a result of constructional changes within the region.

The extreme changing areas emerging as a result of the study indicate the target areas that need to be considered in the development of planning strategies. For an accurate evaluation of the study results, it should be first noted that microclimatic changes occur depending on many factors (number of storeys, floor area, architectural material, afforestation and landscape features, regional texture, traffic structure, energy consumption, etc.). As to constructional changes used in this study are only one of them and of course, the emerging results do not

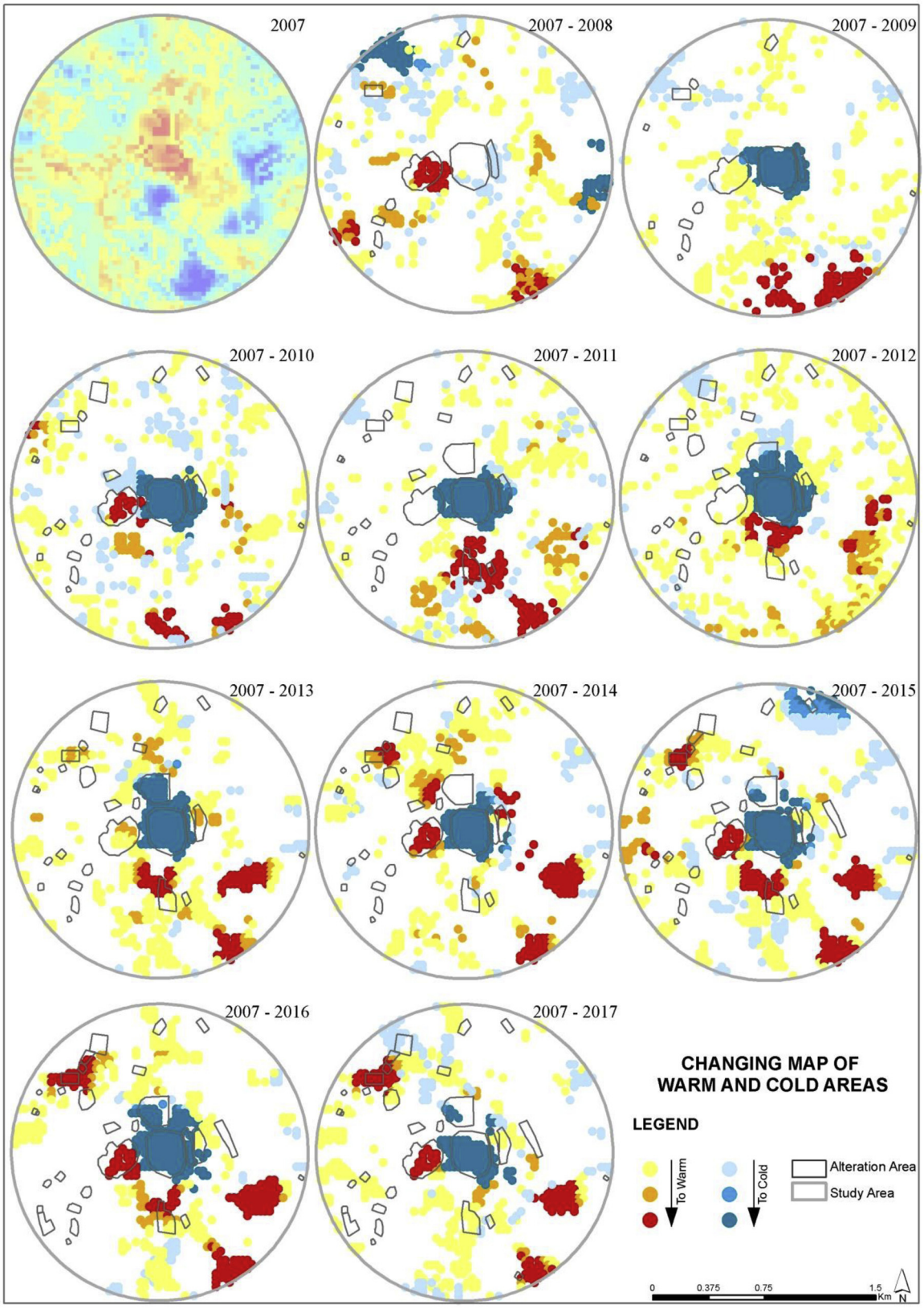

Fig. 4. Changing map of warm and cold areas for Study Area-2.

depend only on this parameter. But, the control of the result maps revealing the climatic changes that took place within a period of 10 years was tested with this way since retrospective terrestrial measurements could not be performed and the data was used which could be reached to perform verification. However, this parameter has a significant relationship with microclimatic changes, as shown by the research findings (Tables 2 and 3). Therefore, it has been accepted based on these results that the model can be used as a control tool.

Table 2
Correlations between overheated/cooled points and their distances with the project areas.

GzScore ≥ -1 (overheated/cooled) and distance with the project area	Years	Spearman's rho			
		Hot points		Cold Points	
		Correlation	Sig(2-tailed)	Correlation	Sig(2-tailed)
Study Area - 1	2007 - 2008	−0.349**	0.000	0.138	0.087
	2007 - 2009	−0.112	0.105	−0.311**	0.000
	2007 - 2010	−0.250**	0.000	−0.388**	0.000
	2007 - 2011	−0.433**	0.000	−0.527**	0.000
	2007 - 2012	−0.442**	0.000	−0.442**	0.000
	2007 - 2013	−0.402**	0.000	−0.317**	0.000
	2007 - 2014	−0.228**	0.002	−0.502**	0.000
	2007 - 2015	−0.344**	0.000	−0.311**	0.000
	2007 - 2016	−0.234**	0.000	−0.342**	0.000
	2007 - 2017	−0.200**	0.002	−0.259**	0.002
Study Area - 2	2007 - 2008	0.338**	0.000	0.072	0.281
	2007 - 2009	0.371**	0.000	−0.700**	0.000
	2007 - 2010	−0.144**	0.008	−0.596**	0.000
	2007 - 2011	−0.038	0.479	−0.784**	0.000
	2007 - 2012	0.131**	0.003	−0.629**	0.000
	2007 - 2013	0.095*	0.034	−0.745**	0.000
	2007 - 2014	−0.151**	0.002	−0.792**	0.000
	2007 - 2015	−0.004	0.933	−0.672**	0.000
	2007 - 2016	0.135**	0.004	−0.756**	0.000
	2007 - 2017	0.056	0.236	−0.778**	0.000

** Correlation is significant at the 0.01 level (2-tailed).

It is known that constructional changes are important for urban climate change (Boukhabla, Alkama, & Bouchair, 2013; Ho, Ren, & Ng, 2015; Levermore et al., 2017; Sebti, Alkama, & Bouchair, 2013). When the climatic changes expected in the region depending on the characteristics of constructional changes in the project area were examined, it was observed that the results that were consistent with the literary information were obtained. The results obtained reveal that there are significant and high correlations between constructional changes and microclimatic changes within the study areas. When the study areas and the projects they contain are discussed separately and evaluated together with the literature data, it is observed that different urban highlights have emerged. In the results of the study, it is observed that two major projects, which are the centers of the study areas, have caused different climatic effects.

The heat absorption in buildings and on surfaces is then spread around and leads to a sensible increase in temperature (Bouchair, 2001; Yang & Li, 2015; Yang, Li, Luo, & Chan, 2016). Similarly, bare soil (without irrigation) creates a higher heating effect compared to surfaces with vegetation cover (Broadbent, Coutts, Tapper, & Demuzere, 2018; Shiflett et al., 2017). When study area-1 is examined, it is observed that the hottest points of the region were gathered within the project area along with the demolition of Ali Sami Yen stadium. The construction became evident in 2014 in the region that turned from the green area into bare soil. During this process, it was observed that the domination of bare soil in the project area created hot areas in the region, in line with the literature. The project started to rise in 2015 and was

Table 3
Correlations between overheated/cooled points and their distances with the project areas.

GzScore ≥ 2 (extreme overheated/cooled) and distance with the project area	Years	Spearman's rho			
		Hot points		Cold Points	
		Correlation	Sig(2-tailed)	Correlation	Sig(2-tailed)
Study Area - 1	2007 - 2008	0.114	0.471	0.357*	0.030
	2007 - 2009	−0.334	0.137	0.345	0.298
	2007 - 2010	0.084	0.605	−0.069	0.718
	2007 - 2011	−0.809**	0.000	0.264	0.248
	2007 - 2012	−0.784**	0.000	0.350*	0.025
	2007 - 2013	−0.725**	0.000	0.302*	0.037
	2007 - 2014	−0.753**	0.005	0.270**	0.000
	2007 - 2015	−0.758**	0.000	−0.453**	0.007
	2007 - 2016	−0.235**	0.000	0.487**	0.000
	2007 - 2017	−0.262	0.082	0.237	0.069
Study Area - 2	2007 - 2008	−0.252	0.071	−0.197	0.098
	2007 - 2009	0.407**	0.000	−0.351**	0.000
	2007 - 2010	−0.415**	0.001	−0.374**	0.000
	2007 - 2011	−0.201	0.072	−0.478**	0.000
	2007 - 2012	−0.252	0.091	−0.494**	0.000
	2007 - 2013	0.133	0.212	−0.577**	0.000
	2007 - 2014	−0.102**	0.003	−0.657**	0.000
	2007 - 2015	−0.050	0.554	−0.467**	0.000
	2007 - 2016	0.012	0.877	−0.616**	0.000
	2007 - 2017	0.194*	0.038	−0.657**	0.000

** Correlation is significant at the 0.01 level (2-tailed).

Table 4
Surface temperature differences between maximum, minimum and mean values of the study area.

Study Area	Surface Temperatures (C°)	2008	2009	2010	2011	2012	2013	2014	2015	2016	2017
Study Area −1	Ts_{avr}	44,57	41,87	37,65	45,65	43,12	44,56	48,34	42,21	41,60	50,85
	Ts_{max}	63,04	57,28	66,54	63,98	60,80	58,39	60,11	58,09	53,20	63,77
	Ts_{min}	35,71	33,88	29,19	36,67	27,84	35,67	37,17	33,35	28,58	41,71
	ΔTs_{max} (Ts_{max}- Ts_{avr})	18,47	15,41	28,89	18,33	17,68	13,83	11,77	15,88	11,6	12,92
	ΔTs_{min} (Ts_{ort} – Ts_{min})	8,86	7,99	8,46	8,98	15,28	8,89	11,17	8,86	13,02	9,14
	ΔTs (Ts_{max}.Ts_{min})	27,33	23,4	37,35	27,31	32,96	22,72	22,94	24,74	24,62	22,06
Study Area −2	Ts_{avr}	41,07	36,80	32,90	39,18	37,95	43,04	34,22	35,61	38,32	40,53
	Ts_{max}	47,83	42,21	38,13	43,90	47,76	46,92	37,86	39,89	42,54	44,63
	Ts_{min}	32,69	31,44	27,17	31,99	28,01	37,80	29,34	29,54	32,12	34,47
	ΔTs_{max} (Ts_{max}- Ts_{avr})	6,76	5,41	5,23	4,72	9,81	3,88	3,64	4,28	4,22	4,1
	ΔTs_{min} (Ts_{ort} – Ts_{min})	8,38	5,36	5,73	7,19	9,94	5,24	4,88	6,07	6,2	6,06
	ΔTs (Ts_{max}.Ts_{min})	15,14	10,77	10,96	11,91	19,75	9,12	8,52	10,35	10,42	10,16

completed in 2016. As the structure began to rise, hot areas began to move towards the south of the project area, and cold areas became evident in the northeastern region. Skyscrapers' shadow effect could cause a cooling around them (Alexandri, 2002; Oke, Mills, Christen, & Voogt, 2017). This cooling occurring with the rise of the structure in the northern part of the project area is a result consistent with the cooling effect of the skyscraper. On the other hand, the regions with a mixture of high and low buildings compared to buildings of a similar height are provide more ventilation (Peng, Wong, Ho, Nichol, & Chan, 2017; Skinner, 2006). Also, green roofs offer a potential to decrease the heat island effects (Lehtihet & Bouchair, 2018). When study area-2 is examined, the extreme cooling region occurring on the project-1 (Zorlu Center) is remarkable. The change that occurred around the building with variable elevation and roof garden is compatible with the cooling effect which was also indicated in the literature.

Dense housing, especially in valley areas, leads to the obstruction of airflow channels, and therefore, the formation of heat islands (Nichol, 2005). This kind of climatic change observed in study area-1 occurred in the region where there are projects number 5-16-22-23. In this region which is located in the valley, along with the start of the constructions, the warming was started, and an extremely hot region was formed after the completion of them. This is consistent with the result that structuring in valley areas clogs the air channels and leads to the formation of heat islands as mentioned in literature.

Furthermore, degraded vegetation texture in urban centers, destruction of green areas, and the increase in dark surfaces create a higher heating effect by increasing heat absorption (Bhatta, 2010; Sungwook et al., 2018). One of the other important climate change observed in this study is the warming caused by the destruction of the green areas. So, these results are consistent with the literature.

The most important situation that should be emphasized here in terms of urbanization is those extremely hot and extremely cold areas can occur within very close distances. This situation that emerged against the constructional changes that took place in the region also reveals that urban geometry has unignorable importance for the urban climate. High-temperature changes occurring at short distances (Table 5) depending on the effect of constructing also lead to the formation of climatic environments that will adversely affect human health within the city. Therefore, it is a necessity to take into account the temperature changes and direction/velocity of wind as climatic features in planning for the formation of healthy cities.

The aim of urban sustainability is to manage resources and to provide services through effective design and implementation of policies, which require access to detailed information on urban indicators. Therefore, data and analyzes are the most important parameters of sustainable urban planning. At this point, remote sensing data provide effective solutions for the monitoring of urban changes by collecting vast amounts of data compared to conventional approaches such as survey and field monitoring (Ali, Marsh, & Smith, 2017; Gaitani, Burud, Thiis, & Santamouris, 2017; Kadhim, Mourshed, & Bray, 2016). Thereby, the use of satellite images in climatic studies is of great importance since it allows obtaining synchronous data on large areas. Furthermore, the fact that retrospective terrestrial measurements cannot be performed makes it essential to use satellite images in regional change analyses. So, although there is a loss of detail or loss of evaluation depending on data acquisition over the surface cover in performing microclimatic research with remote sensing techniques, the only way to reveal the change compared to previous years and to monitor the large area is based on the use of remote sensing techniques. The results obtained from this study shows that moderate-resolution

Table 5
Maximum surface temperature differences in 100 m around of the major project areas.

Study Area	Project No	Maximum surface temperatures differences* (C°)									
		2008	2009	2010	2011	2012	2013	2014	2015	2016	2017
Study Area −1	*3*	9,49	8,14	8,37	12,99	9,42	12,59	8,79	12,31	10,74	11,12
	4	12,34	12,22	11,80	10,81	11,19	10,14	9,04	9,39	8,58	13,32
	6	17,59	19,33	18,35	26,20	20,90	19,40	18,08	23,41	17,32	16,74
	8	–	14,26	13,63	12,61	11,98	11,07	13,44	12,23	11,66	10,56
	12	–	–	–	9,37	25,82	9,37	10,47	10,20	9,51	8,57
	18	–	–	–	15,96	13,30	14,00	12,23	16,36	13,82	13,61
	19	–	–	–	9,04	10,84	8,17	7,43	8,42	19,07	7,86
Study Area −2	*1*	11,76	8,94	8,92	10,28	13,50	7,24	6,55	7,30	7,69	4,80
	2	–	–	3,51	6,45	9,79	3,68	4,23	3,82	4,96	5,59
	5	5,48	4,77	3,01	5,46	7,22	3,27	3,22	3,25	3,71	3,80
	6	3,83	3,63	3,82	4,19	5,62	2,97	2,69	3,43	3,13	4,09
	22	–	–	–	5,14	6,59	2,66	2,38	2,82	2,27	2,11
	23	–	–	–	8,48	5,56	5,37	5,30	5,09	4,21	4,23
	26	–	–	–	–	6,55	3,18	2,68	4,11	5,31	4,51

* Maximum - Minimum in 100 m around of the project areas.

(USGS, 2011) satellite images (e.g. Landsat) are also suitable for monitoring the micro-scale climate changes in urban areas.

5. Conclusion

The data obtained by the method proposed in this study have sufficient sensitivity for the temporal monitoring of the region. By marking the problem points in this way, target points can be determined for more precise investigations. It is even possible to follow the effects of project areas one by one. Furthermore, the causes of change in microclimate can be more easily revealed by cross-examinations to be performed through a more detailed database of the building structure to be prepared (building storey count, floor area, architectural material, afforestation and landscape features, regional texture, traffic structure, energy consumption, etc.). Also, by this method, the microclimatic disturbances due to the anthropogenic effects or other factors can be followed and the target points, which must be intervened, can be determined easily.

This study is a sample examining differentiation between long years within a 1 km perimeter. However, the same method also allows for the examination of climatic changes by being applied at any scale to be determined by the user (1 km, neighborhood, district, urban, region, etc.) or using time series satellite images with a shorter interval. So, the study presents an easy modeling method that can be applied manually with the help of GIS techniques. More importantly, with the help of this model, it is possible to develop an image processing user interface program for monitoring the temporal changing of microclimate from thermal images in future studies.

Urban climate, which is a very complex and extensive subject, is an important research subject for planning approvals. The strategies to be developed against this situation that varies by the climatic characteristics and effects of regions are also different. Therefore, urban and climatic characteristics should be interpreted very well. This also depends on revealing the present situation, change and problem points from past to present properly. The strategies to be developed for sustainable cities should be addressed as a whole, not only with future estimates over today's data but also with the change from past to present.

Arkitera. Informed by Gürkan Yılmaz, E.T. (2013). http://www.arkitera.com/haber/14179/o-gokdelen-yikilacak (Accessed 20 Nov 2018).

Bartlein, P.J. Lecture Notes. (2017). http://geog.uoregon.edu/bartlein/courses/geog495/lec18.html#mahalanobis-distances (Accessed 10 Feb 2017).

Cnnturk. (2011). https://www.cnnturk.com/2011/spor/futbol/04/17/galatasaraylilarin.ali.sami.yene.vedasi/613608.0/index.html (Accessed 29 June 2018).

Cnnturk. (2014). https://www.cnnturk.com/fotogaleri/turkiye/torun-center-havadan-goruntulendi?page=8 (Accessed 29 June 2018).

Corpneed. (2018). https://corpneed.com/istanbul-torun-center/corpneed-torun-center/ (Accessed 29 June 2018).

Emlak Kulisi. (2004). https://emlakkulisi.com/2004-yilinda-karayollarinin-zincirlikuyudaki-arsasi-satisa-cikarilmis/389620 (Accessed 20 November 2018).

Fotomaç. (2018). https://www.fotomac.com.tr/galeri/galatasaray/ali_sami_yen_stadi?page=49 (Accessed 29 June 2018).

USGS, Miller, H.M., Sexton, N.R., Koontz, L., Loomis, J., Koontz, S.R. & Hermans, C., (2011). The Users, Uses, and Value of Landsat and Other Moderate-Resolution Satellite Imagery in the United States—Executive Report, https://pubs.usgs.gov/of/2011/1031/pdf/OF11-1031.pdf (Accessed 30 November 2018).

USGS. (2018). https://landsat.usgs.gov/landsat-8-data-users-handbook-appendix-b (Accessed 20 May 2018)

Zorlu Grup, (2018) http://vesbe.vestelinvestorrelations.com/en/about-us/zorlu-group.aspx (Accessed 20 November 2018).

Appendix A. Supplementary data

Supplementary material related to this article can be found, in the online version, at doi:https://doi.org/10.1016/j.scs.2018.12.035.

References

Alexandri, E. (2002). The effect of green roofs on the urban climate- a quantitative approach. July *Oral Presentation at the Meeting of the PLEA*, 311–316.

Ali, J. M., Marsh, S. H., & Smith, M. J. (2017). A comparison between London and Baghdad surface urban heat islands and possible engineering mitigation solutions. *Sustainable Cities and Society, 29*, 159–168. https://doi.org/10.1016/j.scs.2016.12.010.

Benali, A., Carvalho, A. C., Nunes, J. P., Carvalhais, N., & Santos, A. (2012). Estimating air surface temperature in Portugal using MODIS LST data. *Remote Sensing of Environment, 124*, 108–121.

Bernard, J., Rodler, A., Morille, B., & Zhang, X. (2018). How to design a park and ıts surrounding urban morphology to optimize the spreading of cool air. *Climate, 6*(10), 1–15. https://doi.org/10.3390/cli6010010.

Bhatta, B. (2010). *Causes and consequences of urban growth and sprawl. Analysis of urban growth and sprawl from remote sensing data. Advances in geographic information science.* Berlin, Heidelberg: Springerhttps://doi.org/10.1007/978-3-642-05299-6_2 Chapter 2.

Bouchair, A. (2001). External environmental temperature: Proposed new formulation. *Building Services Engineering Research and Technology, 22*(3), 133–156. https://doi.org/10.1191/014362401701524181.

Boukhabla, M., Alkama, D., & Bouchair, A. (2013). The effect of urban morphology on urban heat island in the city of Biskra in Algeria. *International Journal of Ambient Energy, 34*(2), 100–110.

Broadbent, A. M., Coutts, A. M., Tapper, N. J., & Demuzere, M. (2018). The cooling effect of irrigation on urban microclimate during heatwave conditions. *Urban Climate, 23*, 309–329. https://doi.org/10.1016/j.uclim.2017.05.002.

Chander, G., Markham, B. L., & Helder, D. L. (2009). Summary of current radiometric calibration coefficients for landsat MSS, TM, ETM+, and EO-1 ALI sensors. *Remote Sensing of Environment, 113*, 893–903.

Coutts, A. M., Beringer, J., & Tapper, N. J. (2007). Impact of increasing urban density on local climate: Spatial and temporal variations in the surface energy balance in Melbourne, Australia. *Journal of Applied Meteorology, 46*, 477–493.

Estoque, R. C., Murayama, Y., & Myint, S. W. (2017). Effects of landscape composition and pattern on land surface temperature: An urban heat island study in the megacities of Southeast Asia. *The Science of the Total Environment, 577*, 349–359. https://doi.org/10.1016/j.scitotenv.2016.10.195.

Ferraris, V., Dobigeon, N., Wei, Q., & Chabert, M. (2018). Detecting changes between optical images of different spatial and spectral resolutions: A Fusion-Based Approach. *IEEE Transactions on Geoscience and Remote Sensing, 56*(3), 1566–1578. https://doi.org/10.1109/tgrs.2017.2765348.

Gabriel, K. M. A., & Endlicher, W. R. (2011). Urban and rural mortality rates during heat waves in Berlin and Brandenburg, Germany. *Environmental Pollution, 159*, 2044–2050.

Gaitani, N., Burud, I., Thiis, T., & Santamouris, M. (2017). Aerial survey and in-situ measurements of materials and vegetation in the urban fabric. *Procedia Engineering, 180*, 1335–1344. https://doi.org/10.1016/j.proeng.2017.04.296.

Grimmond, C. S. B., Roth, M., Oke, T. R., Au, Y. C., Best, M., Betts, R., et al. (2010). Climate and more sustainable cities: Climate information for improved planning and management of cities (Producers/Capabilities Perspective). *Procedia Environmental Sciences, 1*, 247–274.

Guo-Yu, R. (2015). Urbanization as a major driver of urban climate change. *Advances in Climate Change Research, 6*, 1–6.

Hadria, R., Benabdelouahab, T., Mahyou, H., Balaghi, R., Bydekerke, L., El Hairech, T., et al. (2017). Relationships between the three components of air temperature and remotely sensed land surface temperature of agricultural areas in Morocco. *International Journal of Remote Sensing, 39*(2), 356–373.

Hao, M., Hua, Z., Li, Z., & Chen, B. (2017). Unsupervised change detection using a novel fuzzy c-means clustering simultaneously incorporating local and global information. *Multimedia Tools and Applications, 76*(19), 20081–20098. https://doi.org/10.1007/s11042-017-4354-1.

Heinonen, J., & Junnila, S. (2011). A carbon consumption comparison of rural and urban lifestyles. *Sustainability, 3*, 1234–1249.

Herrera-Gomez, S. S., Quevedo-Nolasco, A., & Pérez-Urrestarazu, L. (2017). The role of green roofs in climate change mitigation. A case study in Seville (Spain). *Building and Environment, 123*, 575–584. https://doi.org/10.1016/j.buildenv.2017.07.036.

Ho, J. K., Ren, C., & Ng, E. (2015). A review of studies on the relationship between urban morphology and urban climate towards better urban planning design in (sub)tropical regions. July *Oral Presentation at the Meeting of the 9th International Conference on Urban Climate Jointly with 12th Symposium on the Urban Environment*.

Hulley, G., Veraverbeke, S., & Hook, S. (2014). Thermal-based techniques for land cover change detection using a new dynamic MODIS multispectral emissivity product (MOD21). *Remote Sensing of Environment, 140*, 755–765. https://doi.org/10.1016/j.rse.2013.10.014.

Jiménez-Muñoz, J. C., Cristóbal, J., Sobrino, J. A., Sòria, G., Ninyerola, M., & Pons, X. (2009). Revision of the single-channel algorithm for land surface temperature retrieval from landsat thermal-infrared data. *IEEE Transactions on Geoscience and Remote Sensing, 47*(1), 339–349.

Kadhim, N., Mourshed, M., & Bray, M. (2016). Advances in remote sensing applications

for urban sustainability. *Euro-Mediterranean Journal for Environmental Integration, 1*, 1–22.
Katzfuss, M., Hammerling, D., & Smith, R. L. (2017). A Bayesian hierarchical model for climate change detection and attribution. *Geophysical Research Letters, 44*(11), 5720–5728.
Koc, B. C., Osmond, P., & Peters, A. (2018). Evaluating the cooling effects of green infrastructure: A systematic review of methods, indicators and data sources. *Solar Energy, 166*, 486–508. https://doi.org/10.1016/j.solener.2018.03.008.
Lehtihet, M. C., & Bouchair, A. (2018). The impact of extensive green roofs on the improvement of thermal performance for urban areas in Mediterranean climate with reference to the city of Jijel in Algeria. *AIP Conference Proceedings, 1968*, 1. https://doi.org/10.1063/1.5039250.
Levermore, G., Parkinson, J., Laycock, P., & Lindley, S. (2014). The urban heat island in Manchester 1996–2011. *Building Services Engineering Research and Technology, 36*(3), 343–356.
Levermore, G., Parkinson, J., Lee, K., Laycock, P., & Lindley, S. (2017). The increasing trend of the urban heat island intensity. *Urban Climate, 24*, 360–368. https://doi.org/10.1016/j.uclim.2017.02.004.
Lin, P., Lau, S. S. Y., Qin, H., & Gou, Z. (2017). Effects of urban planning indicators on urban heat island: A case study of pocket parks in high-rise high-density environment. *Landscape and Urban Planning, 168*, 48–60.
Linh, N. H. K., & Chuong, H. V. (2015). *Assessing the impact of urbanization on urban climate by remote sensing perspective: A case study in Danang city Vietnam. The international archives of the photogrammetry, remote sensing and spatial information sciences*207–212 XL-7/W3.
Liu, S., Bruzzone, L., Bovolo, F., & Du, P. (2015). Hierarchical unsupervised change detection in multitemporal hyperspectral images. *IEEE Transactions on Geoscience and Remote Sensing, 53*(1), 244–260. https://doi.org/10.1109/tgrs.2014.2321277.
Lu, D., Li, G., & Moran, E. (2014). Current situation and needs of change detection techniques. *International Journal of Image and Data Fusion, 5*(1), 13–38. https://doi.org/10.1080/19479832.2013.868372.
Mackey, C. W., Lee, X., & Smith, R. B. (2012). Remotely sensing the cooling effects of city scale efforts to reduce the urban heat island. *Building and Environment, 49*, 348–358.
Morakinyo, T. E., Dahanayake, K. W. D. K. C., Ng, E., & Chow, C. L. (2017). Temperature and cooling demand reduction by green-roof types in different climates and urban densities: A co-simulation parametric study. *Energy and Buildings, 145*, 226–237. https://doi.org/10.1016/j.enbuild.2017.03.066.
Nsubuga, F. W. N., Botai, J. O., Olwoch, J. M., Rautenbach, C. J. W., Kalumba, A. M., Tsela, P., et al. (2015). Detecting changes in surface water area of Lake Kyoga sub-basin using remotely sensed imagery in a changing climate. *Theoretical and Applied Climatology, 127*(1-2), 327–337. https://doi.org/10.1007/s00704-015-1637-1.
Oke, T. R., Mills, G., Christen, A., & Voogt, J. A. (2017). *Urban climates.* Chapter 5)Cambridge University Presshttps://doi.org/10.1017/9781139016476.
Peng, F., Wong, M. S., Ho, H. C., Nichol, J., & Chan, P. W. (2017). Reconstruction of historical datasets for analyzing spatiotemporal influence of built environment on urban microclimates across a compact city. *Building and Environment, 123*, 649–660. https://doi.org/10.1016/j.buildenv.2017.07.038.
Petkova, E. P., Vink, J. K., Horton, R. M., Gasparrini, A., Bader, D. A., Francis, J. D., et al. (2017). Towards more comprehensive projections of urban heat-related mortality: Estimates for New York City under multiple population, adaptation, and climate scenarios. *Environmental Health Perspectives, 125*(1), 47–55.
Rehdanz, K., & Maddison, D. (2005). Climate and happiness. *Ecological Economics, 52*, 111–125.
Roshan, G., Rousta, I., & Ramesh, M. (2009). *Journal of Geography and Regional Planning, 2*(12), 310–321.
Roy, J., & Pal, S. (2009). Lifestyle and climate change: Link awaiting activation. *Current Opinion in Environmental Sustainability, 1*, 192–200.
Sabnis, G. M. (2011). *Green building with concrete sustainable design and construction.* CRC Press205–252 Chapter 8).
Salata, F., Golasi, I., Petitti, D., de Lieto Vollaro, E., Coppi, M., & Lieto Vollaro, A. (2017). Relating microclimate, human thermal comfort and health during heat waves: An analysis of heat island mitigation strategies through a case study in an urban outdoor environment. *Sustainable Cities and Society, 30*, 79–96. https://doi.org/10.1016/j.scs.2017.01.006.
Sebti, M., Alkama, D., & Bouchair, A. (2013). Assessment of the effect of modern transformation on the traditional settlement' Ksar' of Ouargla in southern Algeria. *Frontiers of Architectural Research Journal, 2*(3), 322–337.
Şen, Z. (2009). *İklim değişikliği, yerel yönetimler ve sektörler.* Su Vakfı Yayınları ISBN:978-975-6455-39-5.
Shiflett, S. A., Liang, L. L., Crum, S. M., Feyisa, G. L., Wang, J., & Jenerette, G. D. (2017). Variation in the urban vegetation, surface temperature, air temperature nexus. *The Science of the Total Environment, 579*, 495–505. https://doi.org/10.1016/j.scitotenv.2016.11.069.
Skinner, C. (2006). Urban density, meteorology and rooftops. *Urban Policy and Research, 24*(3), 355–367.
Sobrino, J. A., Jiménez-Muñoz, J. C., Sòria, G., Romaguera, M., Guanter, L., & Moreno, J. (2008). Land surface emissivity retrieval from different VNIR and TIR sensors. *IEEE Transactions on Geoscience and Remote Sensing, 46*(2), 316–327.
Songchitruksa, P., & Zeng, X. (2010). Getis–ord spatial statistics to identify hot spots by using incident management data. *Journal of the Transportation Research Board, 2165*, 42–51.
Srivanit, M., & Kazunori, H. (2011). The influence of urban morphology indicators on summer diurnal range of urban climate in Bnagkok metropolitan area. *Thailand International Journal of Civil & Environmental Engineering- IJCEE, 11*(5), 34–46.
Sudmant, A., Gouldson, A., Millward-Hopkins, J., Scott, K., & Barrett, J. (2018). Producer cities and consumer cities: Using production- and consumption-based carbon accounts to guide climate action in China, the UK, and the US. *Journal of Cleaner Production, 176*, 654–662.
Tong, S., Wong, N., Tan, C. L., Jusuf, S. K., Ignatius, M., & Tan, E. (2017). Impact of urban morphology on microclimate and thermal comfort in northern China. *Solar Energy, 155*, 212–223.
Tong, S., Wong, N. H., Jusuf, S. K., Tan, C. L., Wong, H. F., Ignatius, M., et al. (2018). Study on correlation between air temperature and urban morphology parameters in built environment in northern China. *Building and Environment, 127*, 239–249. https://doi.org/10.1016/j.buildenv.2017.11.013.
Tornay, N., Schoetter, R., Bonhomme, M., Faraut, S., & Masson, V. (2017). GENIUS: A methodology to define a detailed description of buildings for urban climate and building energy consumption simulations. *Urban Climate, 20*, 75–93.
Tsoka, S., Tsikaloudaki, K., & Theodosiou, T. (2017). Urban space's morphology and microclimatic analysis: A study for a typical urban district in the Mediterranean city of Thessaloniki, Greece. *Energy and Buildings, 156*, 96–108.
Upreti, R., Wang, Z.-H., & Yang, J. (2017). Radiative shading effect of urban trees on cooling the regional built environment. *Urban Forestry & Urban Greening, 26*, 18–24. https://doi.org/10.1016/j.ufug.2017.05.008.
Voogt, J. A., & Oke, T. (1997). Complete urban surface temperatures. *Journal of Applied Meteorology, 36*, 1117–1132.
Wang, Y., & Akbari, H. (2016). Analysis of urban heat island phenomenon and mitigation solutions evaluation for Montreal. *Sustainable Cities and Society, 26*, 438–446. https://doi.org/10.1016/j.scs.2016.04.015.
Wang, C., & Wang, Z. H. (2017). Projecting population growth as a dynamic measure of regional urban warming. *Sustainable Cities and Society, 32*, 357–365. https://doi.org/10.1016/j.scs.2017.04.010.
Wang, Y., Berardi, U., & Akbari, H. (2015). The urban heat island effect in the city of Toronto. *Procedia Engineering, 118*, 137–144.
Wang, Y., Berardi, U., & Akbari, H. (2016). Comparing the effects of urban heat island mitigation strategies for Toronto, Canada. *Energy and Buildings, 114*, 2–19.
Wang, S., Ma, Q., Ding, H., & Liang, H. (2018). Detection of urban expansion and land surface temperature change using multi-temporal landsat images. *Resources, Conservation, and Recycling, 128*, 526–534. https://doi.org/10.1016/j.resconrec.2016.05.011.
Wang, R., Ren, C., Xu, Y., Lau, K. K.-L., & Shi, Y. (2018). Mapping the local climate zones of urban areas by GIS-based and WUDAPT methods: A case study of Hong Kong. *Urban Climate, 24*, 567–576.
Weng, Q., & Quattrochi, D. A. (2007). *Urban remote sensing.* CRC Press Taylor&Francis Group ISBN: 0-8493-9199-7.
Widyasamratri, H., Souma, K., Suetsugi, T., Ishidaira, H., Ichikawa, Y., Kobayashi, H., et al. (2013). A comparison air temperature and land surface temperature to detect an urbanization effect in Jakarta, Indonesia. *34th Asian Conference on Remote Sensing 2013,* 1097–1104.
Wong, N. H., Jusuf, S. K., & Tan, C. L. (2011). Integrated urban microclimate assessment method as a sustainable urban development and urban design tool. *Landscape and Urban Planning, 100*(4), 386–389.
Xu, Y., Ren, C., Ma, P., Ho, J., Wang, W., Lau, K. K., et al. (2017). Urban morphology detection and computation for urban climate research. *Landscape and Urban Planning, 167*, 212–224.
Yahia, M. W., Johansson, E., Thorsson, S., Lindberg, F., & Rasmussen, M. I. (2018). Effect of urban design on microclimate and thermal comfort outdoors in warm-humid Dar es Salaam, Tanzania. *International Journal of Biometeorology, 62*(3), 373–385.
Yang, X., & Li, Y. (2015). The impact of building density and building height heterogeneity on average urban albedo and street surface temperature. *Building and Environment, 90*, 146–156. https://doi.org/10.1016/j.buildenv.2015.03.037.
Yang, X., Li, Y., Luo, Z., & Chan, P. W. (2016). The urban cool island phenomenon in a high-rise high-density city and its mechanisms. *International Journal of Climatology, 37*(2), 890–904. https://doi.org/10.1002/joc.4747.
Zhang, R., Rong, Y., Tian, J., Chen, S., Li, Z., & Liu, S. (2015). A remote sensing method for estimating surface air temperature and surface vapor pressure on a regional scale. *Remote Sensing, 7*, 6005–6025. https://doi.org/10.3390/rs70506005.
Zhu, Z. (2017). Change detection using landsat time series: A review of frequencies, preprocessing, algorithms, and applications. *ISPRS Journal of Photogrammetry and Remote Sensing, 130*, 370–384. https://doi.org/10.1016/j.isprsjprs.2017.06.013.
Zhu, Z., & Woodcock, C. E. (2014). Continuous change detection and classification of land cover using all available Landsat data. *Remote Sensing of Environment, 144*, 152–171. https://doi.org/10.1016/j.rse.2014.01.011.